scientific reports

Check for updates

OPEN

Study on the degradation mechanism of mechanical properties of red sandstone under static and dynamic loading after different high temperatures

Haixiao Lin, Weidong Liu✉, Duan Zhang, Bin Chen & Xinsheng Zhang✉

To study the effect of high temperature on the mechanical properties of red sandstone, YNS600 electro-hydraulic servo universal testing machine and pneumatic separating Hopkinson press bar (SHPB) device were respectively used to conduct static and dynamic load loading tests on red sandstone after 500~1000 ℃ action, and X diffraction detection. The damage pattern and mechanical property index changes before and after high temperature action were compared, and the relationship between mineral composition, microstructure and mechanical parameters of the specimens and temperature was analyzed, and a theoretical model was constructed. With the increase of temperature, the peak strength and elastic modulus under static and dynamic loading decreased significantly, and compared with the static stress-strain curve, the dynamic stress-strain curve did not have an obvious compaction phase, and the mass loss rate, volume expansion rate, and longitudinal wave velocity attenuation rate increased above 600 ℃. Minerals such as zeolite and pyrite within the red sandstone specimen gradually reacted after high temperature. The theoretical model explains the degradation mechanism of the mechanical properties of red sandstone under the action of idealized high temperature. The research results can provide a reliable scientific basis for the assessment and prediction of rock engineering after high-temperature fire.

Keywords Rock damage, Rock stress, Seepage, Coupling

The exploitation of natural resources, the development of geothermal resources, and the construction of underground engineering projects, among other activities, can affect rock properties and, consequently, lead to engineering disasters. The mechanical properties of rocks subjected to high temperatures differ from those observed at room temperature. The mechanical property changes induced by physicochemical processes within the rocks following high-temperature exposure are closely related to temperature.

Currently, research on the mechanical properties of rocks subjected to high-temperature action is primarily focused on the impact of temperature on the static and dynamic mechanical properties of rocks. The influence of temperature on the mechanical properties of rocks in static and dynamic loads is a key area of investigation. The results of the tests demonstrate that Meng[1] et al. conducted uniaxial and triaxial compression tests on limestone subjected to high temperatures ranging from 20 to 800 ℃. Shi[2] conducted uniaxial compression tests on sandstones at varying temperatures and with differing stratigraphies to ascertain the impact of test temperature and stratigraphy on the physical and mechanical properties of the sandstones. Li[3]et al. observed that above 600 °C, granite specimens exhibited a considerable number of conspicuous large cracks and volume expansion, accompanied by a rapid decline in the coefficient of thermal conductivity. Wang[4] et al. employed a modified split Hopkinson compression bar to conduct dynamic compression tests on granite samples at temperatures between 20 and 500 °C. This allowed for a detailed examination of the effects of heating at varying temperatures and impact rates on the mechanical behavior of the granite specimens. Furthermore, a statistical damage ontology model for rocks based on the Weibull distribution was developed, and the factors influencing the model parameters were analysed. The findings indicate that there is a notable influence of strain rate on the augmentation of dynamic compressive strength at elevated temperatures. Wong[5] et al. conducted dynamic

School of Civil Engineering, Henan Polytechnic University, Jiaozuo 454003, China. ✉email: 1123225535@qq.com; 212208020046@home.hpu.edu.cn

uniaxial compression tests on marbles at high temperatures ranging from room temperature to 750 ℃ using a modified Hopkinson Pressure Bar (SHPB) device, which is equipped with a high-temperature oven and can be heated. The results demonstrated that the peak stresses of the heated specimens exhibited a negative correlation with the heating temperature. Shu[6] et al. conducted a cyclic impact loading test on granite at temperatures between 25 and 800 ℃. The aim was to study the thermal effects of dynamic cyclic loading under the action of rock energy dissipation. The Hopkinson pressure bar (SHPB) experimental system was used to carry out the test on heat-treated rocks. The relationships between energy dissipation, energy dissipation rate, impact time, damage mode, and temperature were examined. Mao[7] et al. investigated the mechanical properties of mudstone under the influence of different loading rates, from room temperature to 400 °C. A series of experiments was conducted by Ping[8–11]to investigate the effects of high-temperature cycling on sandstone specimens. The experiments employed eight distinct strain rates and a dynamic single-axis compression test. Moreover, the influence of elevated temperatures, spanning a range of 25 to 1000 °C, on sandstone was examined through the utilization of shock compression tests. The objective of this study was to elucidate the effects of peak stress, strain, and elastic properties on sandstone under thermal conditions. The damage sustained by the model and the test pieces was found to be dependent on the rate at which they were loaded. Six discrete loading rates were employed for the evaluation of sandstone specimens at temperatures ranging from 25 to 800 °C. A one-dimensional dynamic combination loading was employed to test the limestone specimens at different strain rates, to investigate their fracture mechanics performance. The objective of the analysis was to identify the characteristics of the tensile fracture mechanics and energy consumption of the specimens subjected to a pre-applied static load. Furthermore, the analysis sought to examine the correlation between the mechanical properties and the temperature history of the limestone specimens, which were subjected to six distinct levels of shock pressure following heating to 200, 400, and 600 °C.

Furthermore, Zhang[12] examined the internal mineral composition and microstructural alterations of rocks at elevated temperatures by analyzing the physico-mechanical characteristics, energy dissipation, and damage modes of muddy sandstones at diverse temperatures in both air-dried and saturated states. This was accomplished through the use of the RMT-150B Rock Mechanics apparatus and the Split Hopkinson Pressure Bar (SHPB) device. Furthermore, Jin[13] conducted SEM and EDS tests to examine the microstructure of sandstone. Their research employed magnetic resonance imaging, scanning electron microscopy, and uniaxial testing to investigate the micro-composition and mechanical properties of sandstone under different temperatures and cooling modes. Their findings revealed the change rule of sandstone's mechanical properties under water cooling and natural cooling modes. Li[14]examined the damage behavior of sandstone by subjecting it to heat treatment at varying temperatures. Subsequently, they developed a comprehensive, coupled model to elucidate the underlying damage process. Furthermore, scanning electron microscopy (SEM) and X-ray diffraction (XRD) analyses demonstrate that elevated temperatures induce phase transformations of quartz within the rock, thereby imparting substantial alterations in the physical and mechanical properties of the rock material[15–17].

The aforementioned studies have not yet addressed the variability of mechanical properties of red rocks under static and dynamic loading conditions,, nor have they considered the impact of internal mineral composition changes following high-temperature exposure. This paper employs a combination of X-ray diffraction (XRD) and scanning electron microscopy (SEM) techniques to investigate the mineralogical composition and chemical reactions of red sandstone subjected to various temperatures. The combined analysis of mass loss rate, volume expansion rate, and longitudinal wave velocity loss rate of mechanical parameters of red sandstone after high-temperature action reveals the damage mechanism law of high temperature on the mechanical properties of red sandstone. This provides a specific theoretical basis for the exploitation of deep natural resources, the development of geothermal energy resources, and the construction of underground engineering.

Specimen Preparation

In this paper, the experimental red sandstone was sourced from Jiaozuo City, Henan Province, in accordance with the recommendations of the International Society of Rock Mechanics[18]. This sandstone was used for impact tests on cylindrical specimens, with a diameter close to 50 mm and a height ranging from 25 mm to 50 mm. The cylindrical core sizes adopted for the red sandstone specimens were $\Phi 50 \times 100$ mm and $\Phi 50 \times 25$ mm. These were obtained using a rock coring machine, slicer, and double-end smoothing machine, among other equipment.

Firstly, large rock cores were drilled vertically using a drilling machine. Subsequently, the columnar cores were cut to the approximate test sizes using a slicing machine. Finally, the specimen end faces were ground using a double-end smoothing machine to ensure that the unevenness of the two end faces was less than 0.05 mm and that the end face was perpendicular to the specimen axis with an error of less than 0.25°. This ensured that the machining accuracy met the test requirements. The test specimens were all taken from the same batch of rock blocks, and care was taken to avoid any additional damage to the samples.

Use the brushing method to remove dust, mud, and other impurities on the surface of the sample. After cleaning, use clean paper towels to gently dry the sample surface to avoid leaving water residue. Place the cleaned sample in a well-ventilated place without direct sunlight to dry naturally. After drying, the sample should reach a constant weight, i.e. the weight no longer changes with time.

Pack and seal the sample using a ziplock bag. During the packaging process, make sure that the samples are not subject to mechanical damage such as collision. Uniquely identify and number each sample, and store the sealed samples in a dry, cool, well-ventilated area. Ensure the consistency and comparability of the red sandstone test block samples in the experimental process, to improve the reliability and repeatability of the experimental results.

Experimental equipment

In order to minimize the effect of the discrete physical and mechanical properties of the rock on the test results, the OLYMPUS 5077PR ultrasonic pulse tester was used to test the rock samples at similar longitudinal wave velocities by the relevant provisions of the Standard for Testing Methods for Engineering Rocks (GB/T50266-2013)[19], 2013.

The test was performed using a type OLYMPUS 5077PR ultrasonic pulse tester with NI LabVIEW2020 software, probe frequency 0.1～20MHz, 35 MHz wideband receiver, maximum average power of 500mW, and pulse voltage of 400 V. Equation (1) is the formula for calculating the wave velocity, and rock samples with similar longitudinal wave velocity were selected.

$$V=\frac{d}{t} \tag{1}$$

Where V is the wave velocity, d is the sample length, and t is the acoustic signal time interval.

The wave velocity of the test rock sample ranges from 2530 to 2640 m/s.

Zhengzhou Bona Thermal Furnace Co., Ltd. BR-12 N muffle furnace on the red sandstone samples of high-temperature heating, in order to make the specimens heated uniformly, inside and outside the temperature of the same specimens to leave a certain gap evenly placed.Test set to 10 ℃ / min rate of temperature rise, to be the studio temperature to reach the preset temperature of 500, 600, 700, 800, 900, 1000 ℃, respectively, after a constant temperature of 4 h, and the temperature of the studio is not changed.

The temperature range of 500 ~ 1000 °C is a common heating condition of red sandstone, covering the complete process from mild thermal damage to severe degradation of red sandstone, including strength reduction, brittleness increase, crack extension, and so on. The high temperature has a significant effect on the mechanical properties of the rock, which is of strong practical significance. Temperatures higher than 1000 °C and lower than 500 °C were not involved due to the practical considerations of the study and the limitations of the experimental conditions. At 200 ~ 500℃, the red sandstone mainly undergoes thermal expansion and slight dehydration, and the degradation of mechanical properties is small. Above 1000 °C, the rock may melt and the degradation mechanism turns to liquid or semi-liquid behavior. The difficulty of testing increases at extreme temperatures. Although a wider temperature range is not covered, the results in the range of 500 ~ 1000 °C are of high reference value for the degradation mechanism of the properties of rock materials.

As shown in Fig. 1. The maximum temperature inside the furnace is up to 1200 °C. The chamber size is 300 mm x 300 mm x 400 mm.

The static load uniaxial compression test was carried using by a YNS600 microcomputer-controlled electro-hydraulic servo universal testing machine with DH3814 static strain collector in the mechanic's laboratory after high-temperature action, as shown in Fig. 2, and the controlled loading rate was 0.3 MPa/s.

The uniaxial compressive impact loading test adopts the pneumatic separated Hopkinson press bar device of the Impact Mechanics Laboratory of Henan University of Science and Technology to carry out the dynamic impact test on the red sandstone specimen, as shown in Fig. 3. The impact rod, incident rod and transmission rod of the SHPB test device are all made of the same kind of high-strength alloy steel, and the incident rod end is equipped with a waveform shaper, and the impact strength is controlled by the ordinary nitrogen pneumatic pressure controller during the test.

The impact rod, incident rod, transmission rod, and absorption rod of the SHPB test device are all fabricated from the same high-strength alloy steel, with lengths of 400, 2400, 1200, and 1000 mm, material density of 7800 kg/m^3, the elastic modulus of 210 GPa, Poisson's ratio of 0.3, and longitudinal wave speed of 5190 m/s. The impact rod is equipped with a waveform shaper at the end of the incident rod, and an ordinary nitrogen pneumatic controller is used to control the impact strength during the test.

In order to comparatively analyse the influence of high temperature on the dynamic properties of the red sandstone specimens, the SHPB impact compression test should be carried out under the same loading conditions, i.e. the specimens should be loaded with the same incident wave. Before the impact test on each specimen, the impact stroke of the impact bar is strictly controlled to achieve the same impact velocity and load waveform when the same impact air pressure is used for the test, thus ensuring the consistency of the applied impact load.

According to the basic principle of the SHPB test[20], the dynamic stress σ(t), strain Ɛ (t), and strain rate Ɛ (t) of the red sandstone specimen can be obtained by adopting the three-wave method for data processing[21]. The formulae are

$$\sigma(t)=\frac{EA_0\left(\varepsilon_I+\varepsilon_R+\varepsilon_T\right)}{2A_s} \tag{2}$$

$$\dot{\varepsilon}(t)=\frac{C_0\left(\varepsilon_I-\varepsilon_R-\varepsilon_T\right)}{L_s} \tag{3}$$

$$\varepsilon(t)=\frac{C_0}{L_s}\int_0^t\left(\varepsilon_I-\varepsilon_R-\varepsilon_T\right)dt \tag{4}$$

Where: A_0 and A_S are the cross-sectional areas of the specimen and the compression bar, respectively; E is the modulus of elasticity of the compression bar; C_0 and L_S are the ultrasonic velocity and length of the compression bar, respectively; and $Ɛ_I$, $Ɛ_R$ and $Ɛ_T$ are the incident, reflected and transmitted elastic waves, respectively.

Fig. 1. Muffle furnace.

The instrument used for the XRD test was a SmartLab rotary-target X-ray diffractometer, with the test accelerating voltage set at 20 kV, the scanning speed at 10°/min, and the scanning angle ranging from 10°to 80°. Random samples were taken from the crushed specimens, which were then ground using a ball mill, screened through a 200-mesh sieve, and finally, the samples were evenly spread on a tray to start the test, and the diffraction patterns of the samples were obtained and analysed.

Fig. 2. Electro-hydraulic servo universal testing machine.

Analysis of experimental results

Stress-strain curve

The static and dynamic peak strengths of the red sandstone specimens were tested by electro-hydraulic servo universal testing machine and SHPB test system respectively after different temperatures. Figure 4 shows the static stress-strain curve of the red sandstone specimens after different temperatures. Figure 5 shows the dynamic stress-strain curve of the red sandstone specimen after different temperatures.

As shown in Fig. 4, the static typical full stress-strain curves at each temperature are basically divided into four stages: compression, elasticity, yielding and damage. It is shown in Fig. 5 that the dynamic typical full stress-strain curve at each temperature is basically divided into 3 stages of elasticity, yielding and damage. It can be found that different temperature changes have certain effects on rocks under static and dynamic loading.

With the growth of temperature, the deformation of the red sandstone gradually increases, and the compaction stage of the red sandstone under static loading gradually becomes longer, and the red sandstone is thermally damaged under the action of high temperature, so that the internal mineral composition and structure of the rock undergoes significant changes. In the temperature range of 700 ~ 1000 ℃, the stress-strain curve and 600 ℃ before the change in the magnitude of the larger, this is because of the high temperature of 600 ℃ in the internal structure of the rock has undergone a large change in the primary cracks caused by the expansion of the pore space increased. In the compression stage, new cracks start to sprout and develop gradually in the red sandstone, which is shown by the approximately linear relationship of stress-strain curves.

Compaction stage: in this stage, it does not need a lot of stress to produce large deformation, which is related to the original pores and cracks inside the rock in a short time compaction; With the growth of temperature, the pressure-dense stage of sandstone also gradually becomes longer, and the resulting deformation is also larger. This indicates that the sandstone has undergone thermal damage under the action of temperature, which has caused significant changes in the internal mineral composition and structure of the rock.

In the elasticity stage, the internal fissures and micropores of the red sandstone were continuously extruded, the microtissues were not closed in time, and the pores and pores were continuously contracted, resulting in the red sandstone being continuously extruded and compacted. At the same time, with the increase in temperature, the internal structure of the rock was gradually destroyed, and the strength of the cement and mineral particles

Fig. 3. Diagram of pneumatic split Hopkinson lever device.

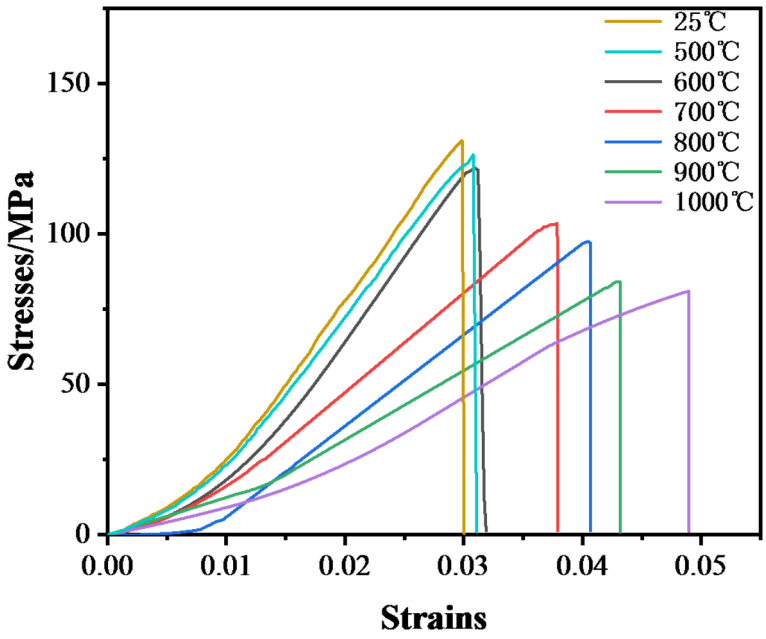

Fig. 4. Static stress-strain curves of specimens after different temperature treatments.

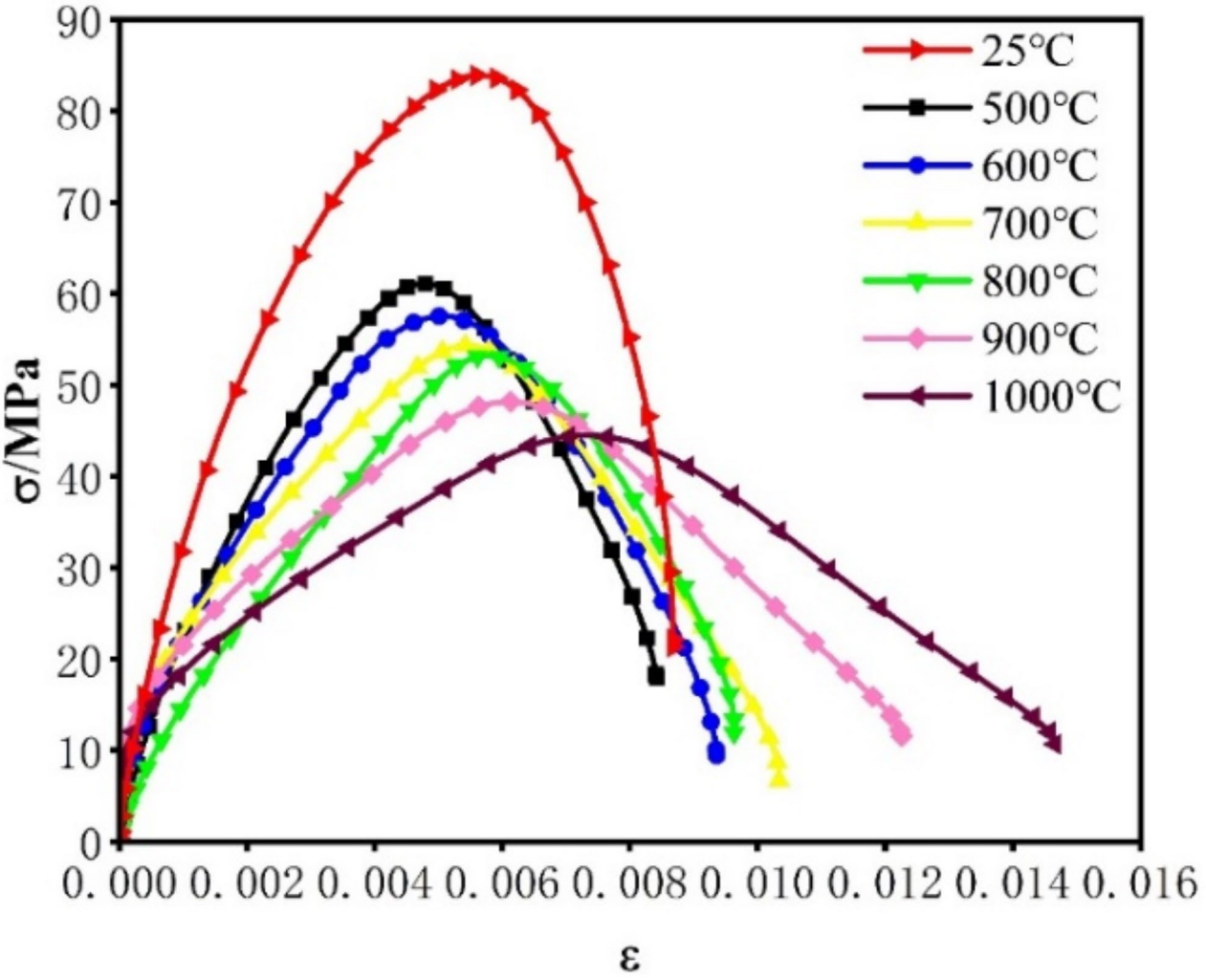

Fig. 5. Stress-strain curves of specimens under impact loading after different temperature treatments.

was reduced, and the slope in the elasticity stage showed a significant decrease, reflecting the effect of high temperature on the rock samples leading to the weakening of the deformation resistance.

In the yield stage, the internal cracks of the rock gradually expand, new cracks continue to be generated, the slope of the curve gradually decreases, and after reaching the yield point, as the internal cracks continue to expand and extend, the main cracks through the specimen are eventually formed. In which the stress acting on the red sandstone specimen by the impact load is lower than the yield strength of the red sandstone, forming an elastic stress wave, the stress at this stage varies linearly with the strain.

In the destructive stage, after the rupture of the rock specimen occurs, the overall bearing capacity decreases rapidly with the increase of strain, and the rock specimen is completely destroyed and loses its bearing capacity. In this stage, the stress of the red sandstone specimen decreases rapidly from the peak state, and the compressive strength of the red sandstone specimen is not enough to resist external force and damage. At 1000 ℃, the strength of the red sandstone specimen is lower, compared with the strength of the red sandstone specimen at 25 to 800 ℃, there is a significant decrease.

From the static and dynamic stress-strain curves of the red sandstone, it can be seen that with the increase in temperature increases the internal damage of the rock samples, resulting in the slope and peak point of the elastic phase of the reduced, these two values reflect the deformation resistance and load-bearing capacity of the rock under static and dynamic loading.

In order to understand the effect of high temperature on the static and dynamic deformation resistance and bearing capacity of rocks, the evolutionary characteristics of peak stress and deformation modulus need to be further analysed.

Peak stress

Figure 6a shows the graph of dynamic load peak stress data of red sandstone after different temperature effects; Fig. 6b shows the graph of static load peak stress data of red sandstone after different temperature effects. According to the experimental and variance data in the figure, it can be clearly seen that near the temperature

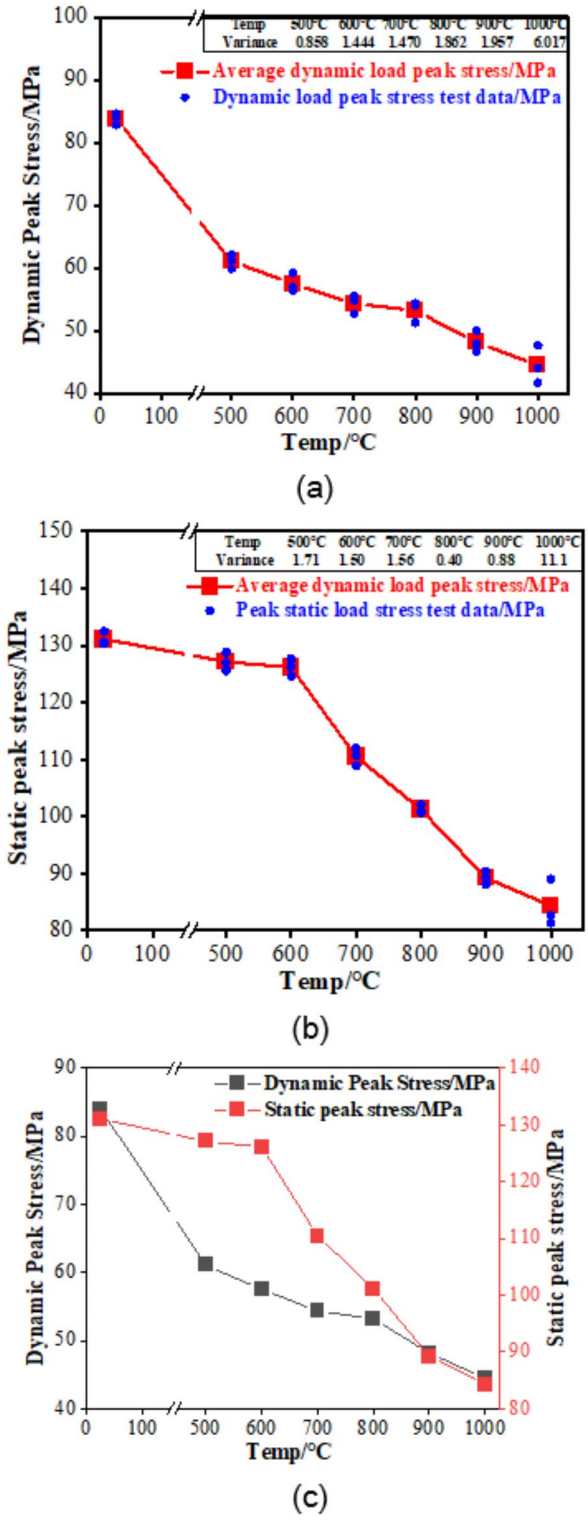

Fig. 6. Plot of peak stress versus temperature in red sandstone after different temperature treatments. (**a**) Peak dynamic load stress data at different temperatures. (**b**) Peak static load stress data at different temperatures. (**c**) Comparison of peak stresses for dynamic and static loads.

of 500 ~ 600℃, the variance becomes larger and the specimen dispersion increases. About 900 ~ 1000℃, the variance again becomes significantly larger and the specimen dispersion increases. This phenomenon reflects that there is a significant difference between the different temperature groups of red sandstone, and these two intervals are the key temperature points for various damage mechanisms, such as mineral phase transformation, melting, dehydration or decomposition, triggered by high temperature.

Use the average of the two data as the peak stress value. Figure 6c shows the comparison of the peak strength patterns of red sandstone specimens under static and dynamic loading after different temperatures. The peak strengths of the two loading cases both decrease significantly with the increase in temperature, and the relationship is basically linear.

The peak stress can be used to characterize the maximum bearing capacity of the rock. As the temperature increases, the static and dynamic peak values of the rock show a decreasing trend. Under static loading conditions, the peak stress reached 131.09 MPa at room temperature, decreased to 127.1 MPa after heating treatment at 500 °C, and reached 84.3 MPa after continuous heating to 1000 °C, with a decrease of 35.6%. Under dynamic loading, it reaches 83.93 MPa at room temperature, the peak stress decreases to 61.07 MPa after heating treatment at 500 °C, and reaches 44.45 MPa after continuous heating to 1000 °C, with a decrease of 47%.

During the process of temperature increase, the attached and bound water within the rock volatilizes at different temperatures, and the corresponding mineral particles and cementation undergo swelling damage.

Modulus of elasticity

Figure 7a shows the dynamic load elastic modulus data of red sandstone after different temperatures, and Fig. 7b shows the static load elastic modulus data of red sandstone after different temperatures. According to the experimental and variance data in the figure, it can be clearly seen that, similar to the case of peak stress near 500 ~ 600℃ and 900 ~ 1000℃, the variance becomes significantly larger and the specimen dispersion increases. Both reflect the internal changes of the red sandstone after suffering from different temperatures have obvious differences.

Taking the average data of both as the elastic model value. The temperature dependence of the modulus of elasticity of the red sandstone under static and dynamic loading after different temperature treatments is shown in Fig. 7c. The mentioned modulus of elasticity is the maximum value of the stress-strain ratio in the stress-strain curve of the red sandstone after treatment with the corresponding calibrated temperature, which is expressed as the deformation-resisting ability of the red sandstone in the test.

With the increase of heating temperature, the elastic modulus of red sandstone treated at high temperature showed an overall decreasing trend. Under static loading conditions, the elastic modulus decreased to 70 GPa after heating treatment at 500 °C and reached 22.5 GPa after continuous heating to 1000 °C. Comparing 500 °C, the decreased rate reaches 71.1%, and the elastic modulus from 500 to 1000 °C were 70, 55, 33, 30, 23, and 22.5 GPa, respectively. Under dynamic loading, the modulus of elasticity decreased to 12.74 GPa after heating treatment at 500 °C, and reached 6 GPa after continuous heating to 1000 °C, with a decrease of 53%. The modulus of elasticity was 12.75、10.87、9.93、8.43、7.85 and 6.09 GPa from 500 °C to 1000 °C, respectively.

The linear modulus of elasticity is minimal when the temperature is 1000 °C. This is mainly caused by the thermal damage effect and its degree of damage increases with the increase of temperature. This reflects that high-temperature treatment gradually destroys the main load-bearing structures such as mineral particles and cement structure within the red sandstone, and the microcracks within the specimen gradually increase, resulting in the degradation of its deformation resistance. Therefore, thermal damage can change the dynamic mechanical properties of red sandstone.

Physical properties of red sandstone after high temperature

Changes in specimen appearance characteristics

The apparent color of the rock is related to the internal mineral composition of the rock, when the red sandstone is treated with different temperatures, its internal composition will undergo a certain transformation, which will lead to changes in the apparent color of the red sandstone. Generally, quartz is gray-white, orthoclase is generally flesh-red, light yellow-red, light yellow-white, plagioclase is milky-white, and calcite is generally white or milky-white. It changes as the temperature rises, and when the temperature exceeds 500 °C, the color changes to light brown. When the temperature increases from 25 to 200 °C, the uniformity of the sandstone grains remains unchanged, and no obvious microcracks appear on the surface.

The damage characteristics of high-temperature sandstone can also reflect its strength characteristics. Figure 8 shows the apparent color of static-loaded red sandstone specimens after high-temperature treatment, Fig. 9 shows the apparent color of dynamically-loaded red sandstone specimens after high-temperature treatment, Fig. 10 shows the experimental damage morphology of the red sandstone at room temperature under static load conditions and after different high-temperature treatments, and Fig. 11 shows the experimental damage morphology of the red sandstone at room temperature under dynamic load conditions and after different high-temperature treatments.

The color of the red sandstone is greyish-white at room temperature. Upon exposure to temperatures over 25 °C, the intergranular voids and particle separation that occur as a result of the temperature increase lead to the formation of prominent granular properties. At temperatures between 500 and 700 °C, the surface of the red sandstone assumes a white-red hue. At temperatures exceeding 600 °C, pronounced microcracks emerge on the surface of the sample. As the temperature continues to increase, reaching 800 ~ 1000 °C, pyrite reacts with oxygen to form hematite. This reaction causes the color of the red sandstone to gradually change from brownish red to bright red.

The degree of crushing under pressure, both under static and dynamic loading, is closely related to temperature. The degree of fragmentation of the red sandstone specimen subjected to static loading increases gradually with the temperature, accompanied by a conical shape of the shear surface and the presence of powdery material on the shear rupture surface, along with clear friction traces. Additionally, part of the specimen displays a longitudinal fracture. Cracks are observed to align with the direction of loading, and the damage morphology of the specimen becomes increasingly complex with the increase in temperature. It is observed that as temperature increases, specimen damage becomes more severe, and the resulting fragmented rock is smaller

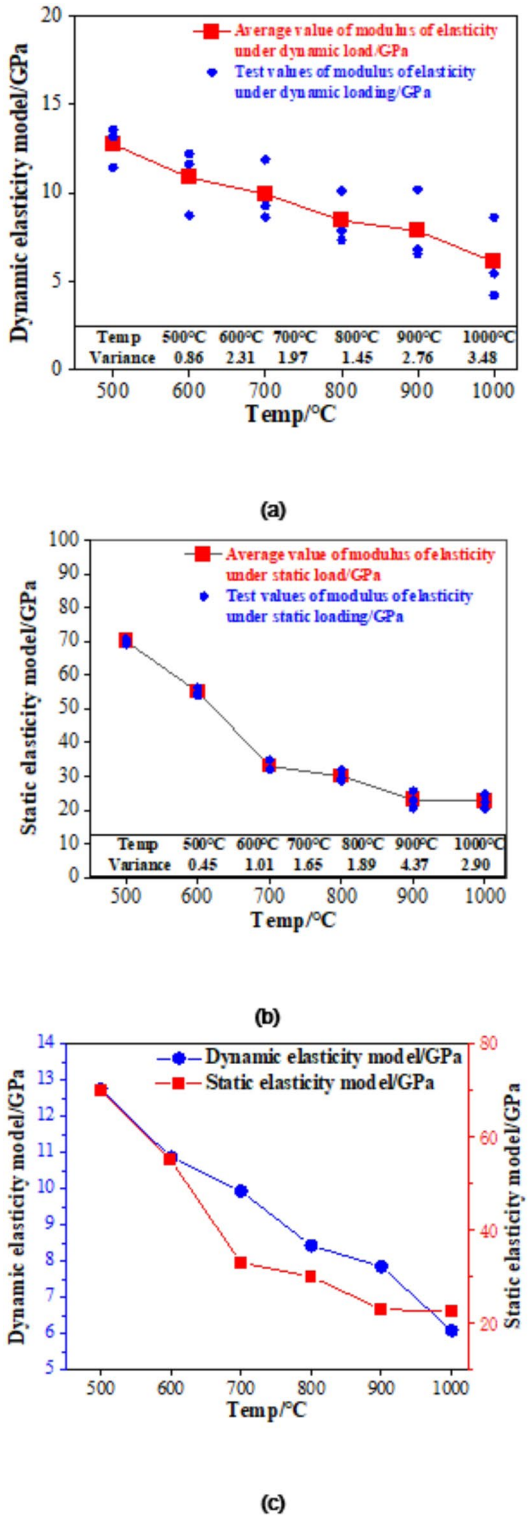

Fig. 7. Plot of elastic modulus versus temperature for red sandstone after different temperature treatments. (**a**) Modulus of elasticity for dynamic loads at different temperatures. (**b**) Modulus of elasticity for static load at different temperatures. (**c**) Comparison of modulus of elasticity for dynamic and static loads.

in size, exhibiting a powdery and crumbly texture. The damage pattern of specimens under dynamic loading becomes increasingly complex with increasing temperature.

The degree of crushing of the specimens under dynamic loading demonstrated a tendency to decrease and then gradually increase with the temperature rise. At a temperature of 25 °C, the red sandstone specimen exhibited a cleavage surface along its axial direction and subsequently fractured into multiple pieces. At temperatures of

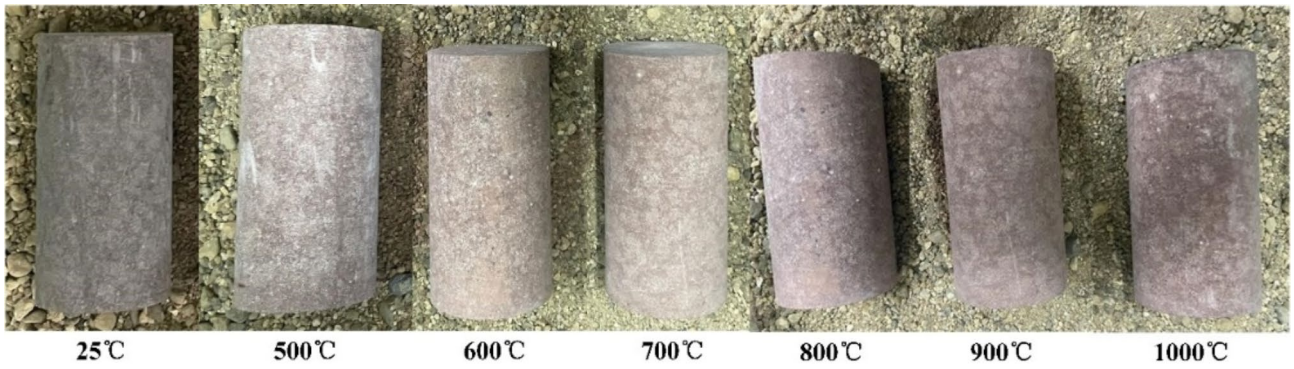

Fig. 8. Apparent colour of static loaded red sandstone specimens after high-temperature treatment.

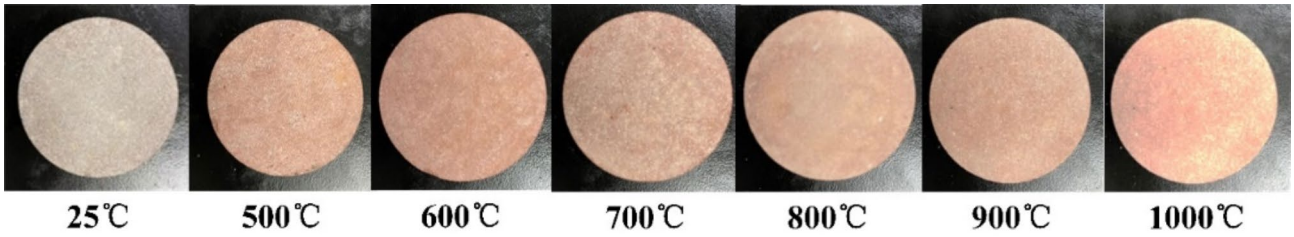

Fig. 9. Apparent colour of dynamically loaded red sandstone specimens after high-temperature treatment.

Fig. 10. Damage fragmentation diagram of red sandstone specimen under static loading after high-temperature action.

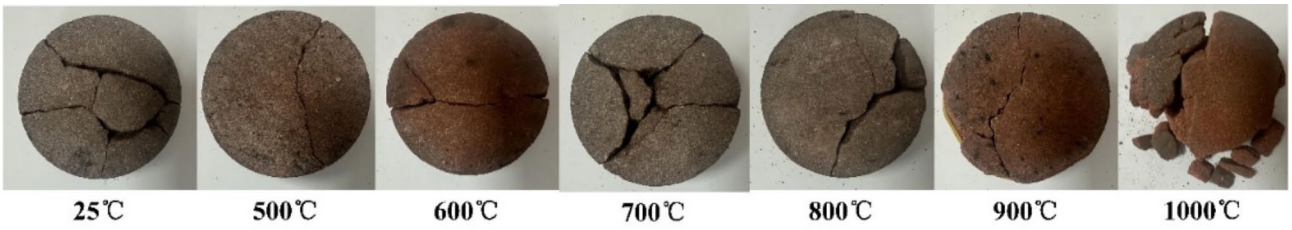

Fig. 11. Damage fragmentation diagram of red sandstone specimen under dynamic loading after high-temperature action.

500 °C and 800 °C, the rupture degree of the specimen did not diminish; conversely, the specimen's dynamic compressive strength increased.

Therefore, the specimen by the impact of the degree of fragmentation with the increase in the action of the temperature shows the trend of the first decrease and then gradually increase. The temperature of 900 ℃

or more, the emergence of axial cleavage surface, specimen damage began to intensify, 1000 ℃, the specimen broken into smaller pieces.

Effect of high temperature on specimen mass, volume and longitudinal wave velocity

The application of elevated temperatures results in the evaporation and loss of diverse water types within the rock. This occurs at a specific temperature and is accompanied by phase transformation and the decomposition, dehydroxylation, and other physicochemical reactions of minerals. These changes impact the quality, volume, and density of the rock, influencing its mineral composition and pore space development. Consequently, the longitudinal wave velocity of the rock undergoes alteration. Consequently, the extent of damage to red sandstone following exposure to high temperatures can be gauged by examining the fluctuations in mass loss rate, volume expansion rate, and longitudinal wave velocity. As illustrated in Fig. 12, the mass loss rate, volume expansion rate, and longitudinal wave velocity attenuation rate of the specimen subjected to high temperatures are presented about the temperature.

The mass loss rate of the red sandstone specimen increases at a relatively slow rate between 500 and 700 °C, reaching a value of 1.81% at 700 °C. This is due to the evaporation of free and bound water within the red sandstone, which results in a reduction in the specimen's mass. At temperatures between 700 and 1000 °C, the rate of mass loss accelerates significantly. During this phase, the mass loss rate increases from 1.81 to 5.76%. This rapid growth stage is characterized by a more complex mass reduction process. In addition to the decomposition of calcite to produce CO_2 and facilitate escape, there are also processes of mineral decomposition, phase change, and dehydroxylation, including mineral detachment, phase change of quartz, and dehydroxylation reaction of kaolinite, among others.

The volumetric expansion of red sandstone specimens in the 500 to 1000 °C stage with increasing temperature is due to the differences in the coefficients of thermal expansion of the different mineral compositions within the red sandstone. This results in the generation of thermal cracks, which subsequently expand the volume. In the temperature range of 500 to 800 degrees Celsius, the volume expansion rate of red sandstone exhibits a relatively gentle increase, reaching approximately 1.5% with each degree Celsius rise. However, as the temperature continues to increase, the volume expansion rate accelerates significantly, reaching 3.5% at 1000 degrees Celsius. As the temperature rises, the water vapor pressure inside the rock gradually increases, which in turn accelerates the expansion of the cracks. This process results in a rapid increase in volume. Additionally, the process of mineral phase change also accelerates the shedding of mineral particles. Concurrently, during the cooling phase, the cracking phenomenon will result in the formation of additional microfractures, thereby increasing the volume of the red sandstone.

The longitudinal wave attenuation rate of red sandstone exhibits a linear increase between the temperatures of 500 and 1000 °C. The change in the rate is also approximately linear, with a decrease from 35% at 500 °C to 76.92% at 1000 °C. This indicates that the velocity of the wave decreases gradually as the temperature rises. Following the application of high temperatures, a series of physical and chemical reactions, including dehydration, phase change, melting, crack development, and differential mineral expansion, occur within the rock. These reactions result in alterations to the rock's density, mineral composition, and pore development, which in turn affect the longitudinal wave velocity of the rock.

High temperatures can cause thermal expansion of red sandstone grains, resulting in tiny gaps between otherwise tightly packed grains, thus increasing the overall porosity of the rock. In addition, high temperatures may cause phase changes or decomposition of minerals within the rock, creating new pores or cracks and further increasing porosity.

Increased porosity means an increase in the number of fluid passages within the rock, thus increasing the permeability of the rock. The connectivity of the pores and cracks inside the rock increases. Therefore, the increase in porosity of red sandstone at high temperatures directly leads to an increase in its permeability.

Under the action of high temperature and stress loading, the rock is more prone to volume expansion and plastic deformation during the loading process due to the increase in porosity and volume expansion rate. This deformation leads to a reduction in the bearing capacity of the rock and makes it more susceptible to damage.

Under the effect of high temperature and osmotic pressure, the enhancement of permeability of red sandstone can make it easier for fluids to flow inside the rock, thus accelerating the creep process of the rock. This may result in rocks being more susceptible to deformation and damage under long-term loading.

Therefore, the influence of these factors on the mechanical behavior of rocks needs to be fully considered in rock engineering in high-temperature environments to ensure the safety and stability of the project.

Mineral composition of specimen

Under heat-treatment conditions, the periodicity of the crystals is somewhat disrupted, generating additional phase differences that lead to incomplete phase-length interference under Bragg-compliant conditions. As a result, the diffraction intensity changes. According to the results of X-ray diffraction experiments, the X-ray diffraction patterns of red sandstone at room temperature and in the range of 500℃~1000℃ are plotted, as shown in Fig. 13 The main mineral compositions of the red sandstone used in this experiment are quartz, sodium feldspar, and a small amount of clay and so on. Figure 14 shows the X-ray diffraction information of the red sandstone after the action of different temperatures. The diffraction peaks of zeolite disappeared before heating to 500 °C. Pyrite reacted with oxygen to form hematite at 600 °C ~ 1000 °C, which led to a gradual change in the color of the red sandstone to brownish red and bright red. Plagioclase pyroxene and the diffraction peak disappear at 700℃, montmorillonite disappear at 900℃, while quartz, sodium feldspar, hornblende, etc. are relatively stable.

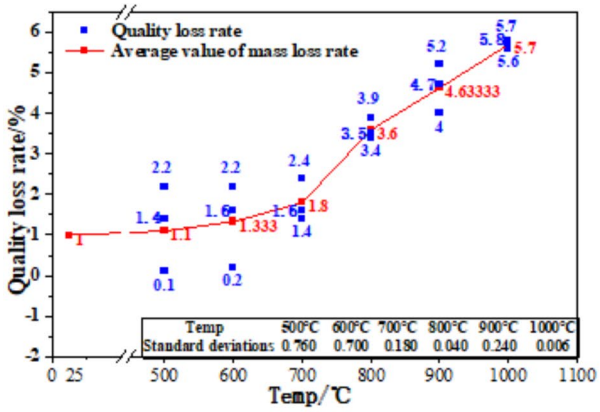

(a)

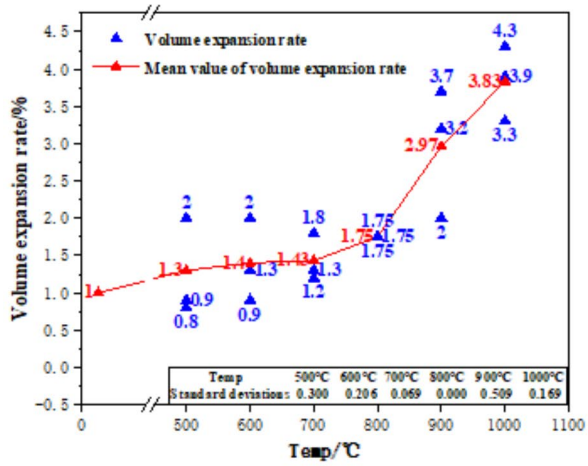

(b)

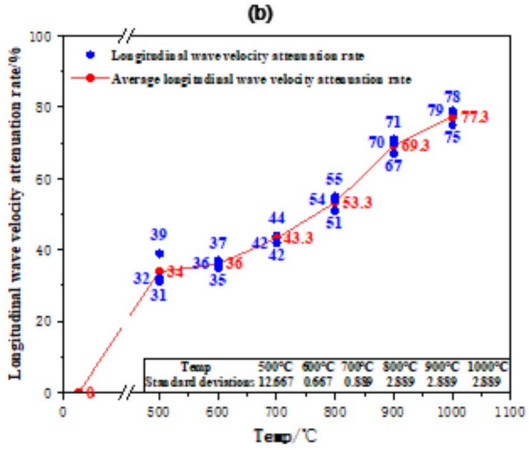

(c)

Fig. 12. Mass loss rate, volume expansion rate and longitudinal wave velocity attenuation rate of specimen after high temperature versus temperature. (**a**) Mass loss rate as a function of temperature. (**b**) Volume expansion versus temperature. (**c**) Longitudinal wave attenuation rate versus temperature.

(1) The chemical composition and structure of square zeolite ($NaAlSi_2O_6 \bullet H_2O$) varies according to species but usually contains elements such as silicon, aluminum, oxygen, etc. The zeolite in the red sandstone of this experiment is square zeolite. Its diffraction peak disappears when the temperature rises to 600 ℃, indicating that the decomposition of square zeolite occurs at a certain temperature before 600℃. When the

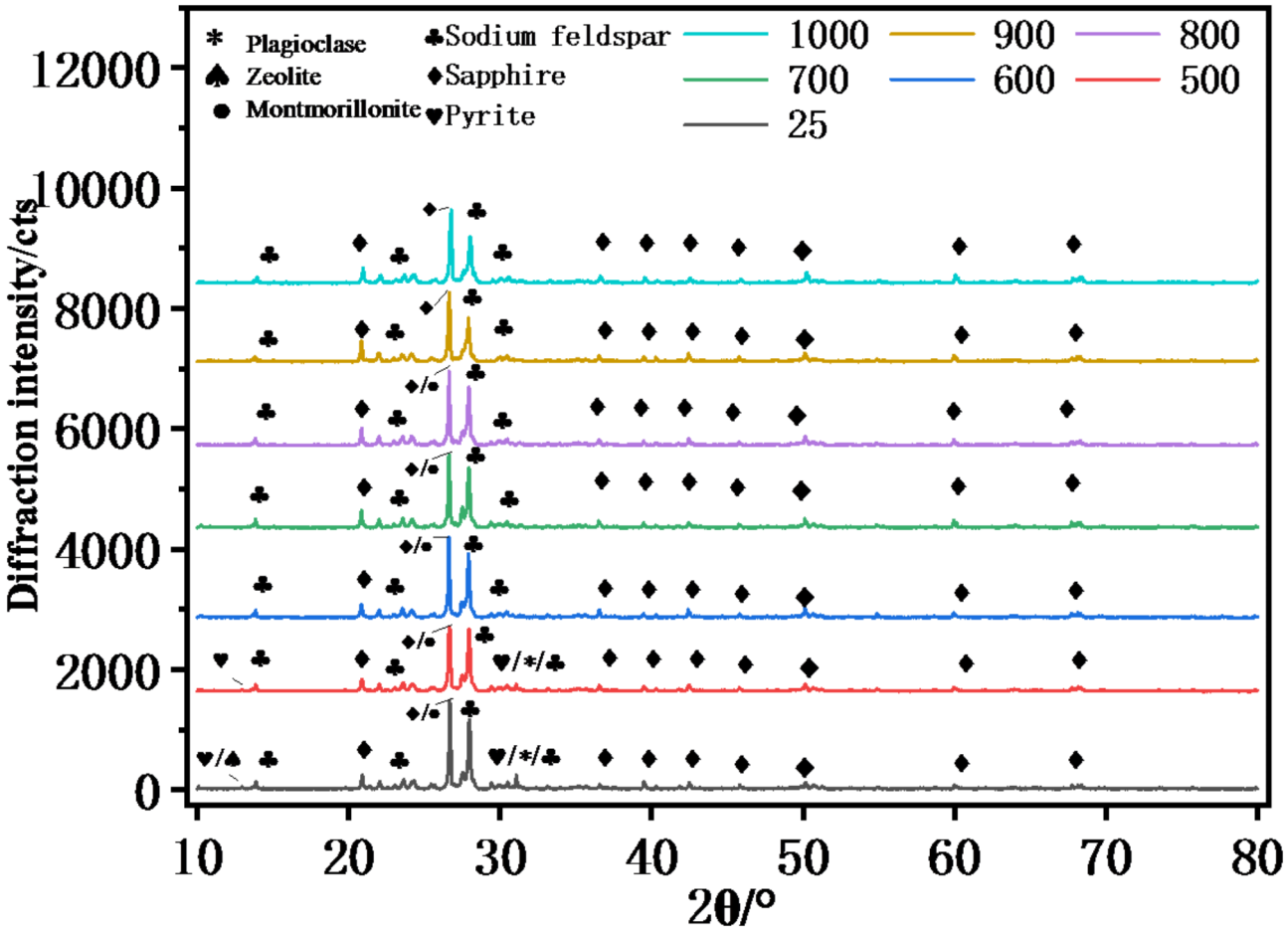

Fig. 13. X-ray diffraction patterns of red sandstone at different temperatures.

decomposition is completed before 600 ℃, its decomposition generates silica, aluminum oxide, oxide Na, and other substances, the equation is:

$$NaAlSi_2O_6 \cdot H_2O \rightarrow 2SiO_2 + Al_2O_3 + Na_2O + H_2O \quad (5)$$

Square zeolite loses its water of crystallization at high temperatures, leading to changes in its structure. This in turn produces microcracks or pores within the rock, thus affecting the mechanical properties of the rock.

(2) Plagioclase ($(Mg, Fe)_2[Si_2O_6]$) is a silicate mineral whose chemical formula can be expressed as $MgSiO_3$. decomposition reaction can occur at high temperatures, in the experiment plagioclase can still be observed at 600 ℃ diffraction peaks, diffraction peaks disappeared at 700 ℃, indicating that in the temperature interval, the decomposition of plagioclase occurs, and its decomposition generates olivine, silica, siderite, and other and other substances, whose equations are:

$$Mg_2Si_2O_4 \rightarrow Mg_2SiO_4 + SiO_2 \quad (6)$$

$$Fe_2Si_2O_6 \rightarrow 2SiO_2 + 2FeO \quad (7)$$

Plagioclase pyroxene undergoes reactions such as thermal expansion, thermal decomposition or phase transformation at high temperatures. The creation of microcracks or pores within the rock leads to stress concentrations within the rock, which reduces the strength and modulus of elasticity of the rock.
In addition, the coefficient of thermal expansion of plagioclase may be different from that of the surrounding minerals, leading to the generation of thermal stresses inside the rock, further aggravating the damage to the rock.

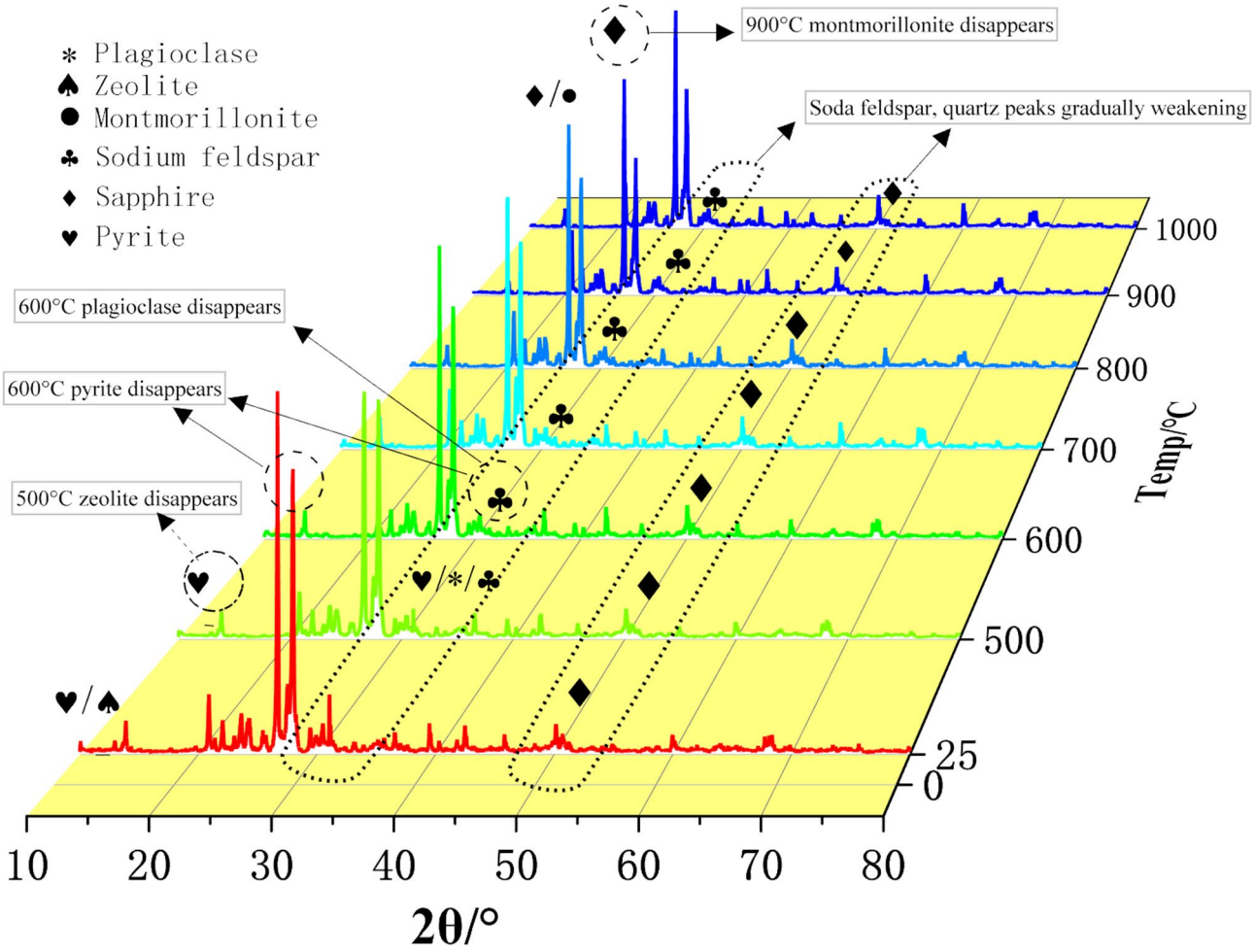

Fig. 14. X-ray diffraction waterfall.

(3) Montmorillonite ($CaAl_4Si_8O_{20}(OH)_4 \bullet nH_2O$)is a layered silicate clay mineral, which is mainly composed of silicon, aluminum, oxygen and other elements, and contains a small amount of water molecules and exchangeable cations. Calcium montmorillonite is found in the red sandstone in the experiments, and the first heat-absorption valley occurs between 80 and 250 °C to shed interlayer water and adsorbed water; the second heat-absorption valley occurs Between 600~700℃,de-structured water; the third heat absorption valley at 800 ~ 935 ℃, the lattice is destroyed, the equation is:

$$CaAl_4Si_8O_{20}\,(OH)_4 \cdot nH_2O \rightarrow CaO + 2Al_2O_3 + 8SiO_2 + \ nH_2O \tag{8}$$

Montmorillonite is a layered silicate mineral with strong hydrophilicity. At high temperatures, montmorillonite undergoes dehydration, leading to changes in its interlayer structure and a decrease in the interlayer distance, which reduces the densification of the rock and produces more microcracks and pores inside the rock, thus affecting the mechanical properties of the rock and showing that dehydrated montmorillonite is more susceptible to crushing.
In addition, the expansion of montmorillonite at high temperatures may also lead to cracks or pores inside the rock, reducing the strength and elastic modulus of the rock.

(4) Feldspar ($NaAlSi_3O_8$) is an aluminosilicate mineral with a stable crystal structure, and kaolinite ($Al_4Si_4O_{10}(OH)_8$) feldspar, common pyroxene, and other aluminosilicate minerals are formed by weathering and have good refractory properties, and the diffraction intensity decreases consistently between 500 °C and 1000 °C due to the effect of loss of water in the structure and the chemical equations, respectively:

$$NaAlSi_3O_8 \rightarrow Na_2O + Al_2O_3 + 3SiO_2 \tag{9}$$

$$Al_2Si_2O_5(OH)_4 \rightarrow Al_2O_3 + 2SiO_2 + 2H_2O \tag{10}$$

Sodic feldspar undergoes thermal decomposition reactions at high temperatures to produce products such as alumina, silicon oxide, and sodium oxide. The physical and chemical properties of these products are different from those of sodium feldspar, which may lead to changes in the internal structure of the rock, thus affecting the mechanical properties of the rock. In addition, the coefficient of thermal expansion of sodium feldspar may also be different from that of the surrounding minerals, leading to thermal stresses within the rock.

Kaolinite is a layered silicate mineral that undergoes dehydration at high temperatures, leading to changes in its structure. In particular, when the temperature reaches 470～520°C, kaolinite will shed the (OH) in the outer layer of its structure, and when the temperature reaches 540 °C, the (OH) in the inner layer of the structure will also be shed, resulting in serious damage to the structure of kaolinite. This dehydration may lead to changes in the internal pore structure of the rock, thus reducing the strength and elastic modulus of the rock.

Dehydrated kaolinite may be more susceptible to chemical reactions, such as replacement reactions with surrounding silicate minerals, to produce new mineral phases, which may have lower strength and elastic modulus.

(5) Pyrite (FeS_2)decreases slowly at 600 ~ 1000 °C, when pyrite reacts with oxygen to form hematite, thus gradually changing the color of the specimen to brownish red and bright red. The chemical equation is:

$$4FeS_2 + 11O_2 \rightarrow 2Fe_2O_3 + 8SO_2 \tag{11}$$

Pyrite undergoes oxidation at high temperatures to produce products such as iron oxide and sulfur dioxide. This oxidation may lead to changes in the chemical composition and structure within the rock, thereby affecting the mechanical properties of the rock. At the same time, gases such as sulfur dioxide produced by oxidation may escape through microcracks in the rock, further exacerbating the damage to the rock. In addition, the oxidation of pyrite may produce volume expansion, leading to cracks or pores within the rock.

In addition, the two Si-O chemical bonds in the α-quartz structure are at an angle of 150°. When the quartz sand is heated to 573 °C the α-quartz is transformed into β-quartz, and the two Si-O chemical bonds in the β-quartz structure are at an angle of 150°, and the value of the diffraction intensity is still lower than that of the initial temperature, which indicates that the temperature action also has a damaging effect on the crystal structure of the quartz, which produces irreversible changes, as shown in Fig. 15[15].In addition, at 500 °C, OH- and H- will separate from the mineral skeleton, and the loss of component water and water of crystallization will lead to further damage to the mineral crystal structure[22]. At this time, the internal microcracks of the red

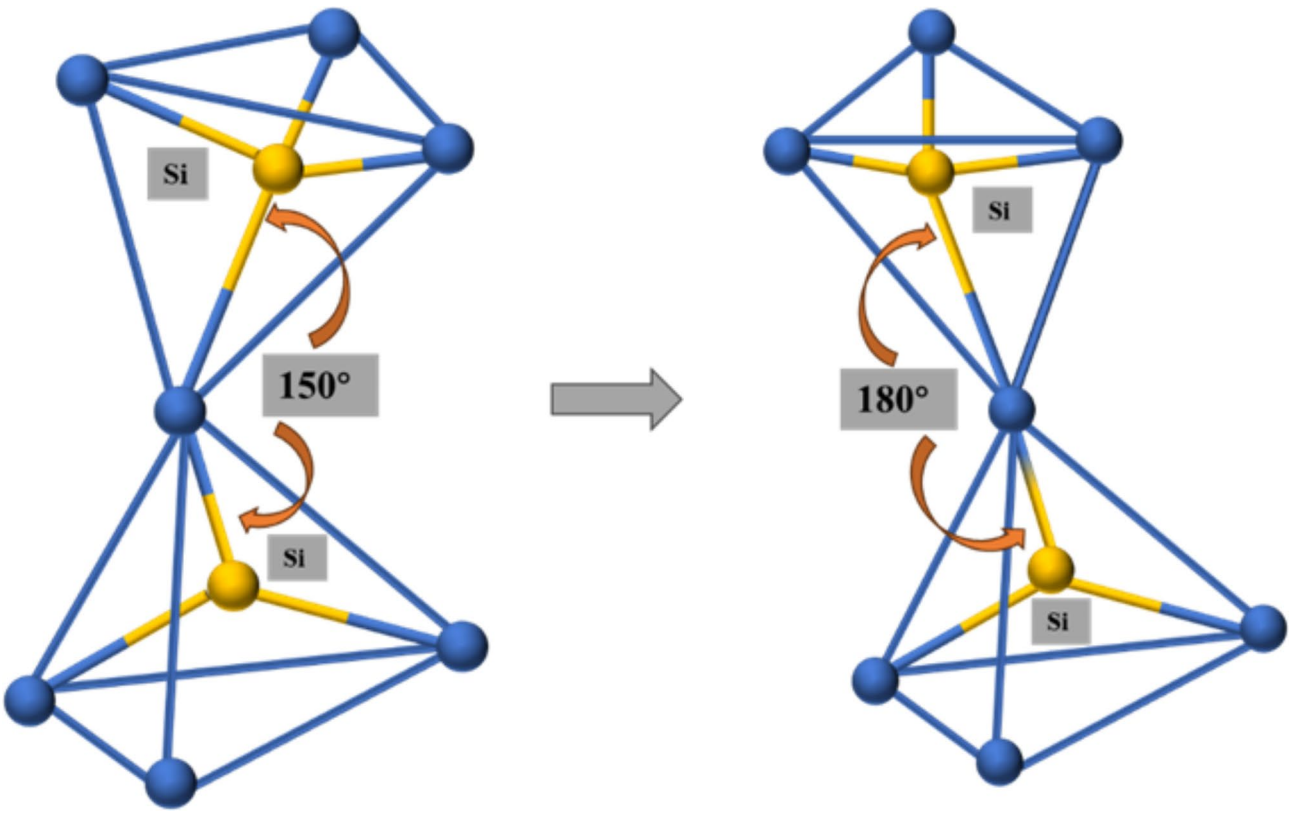

Fig. 15. Schematic diagram of the variation of α-β quartz bond angle.

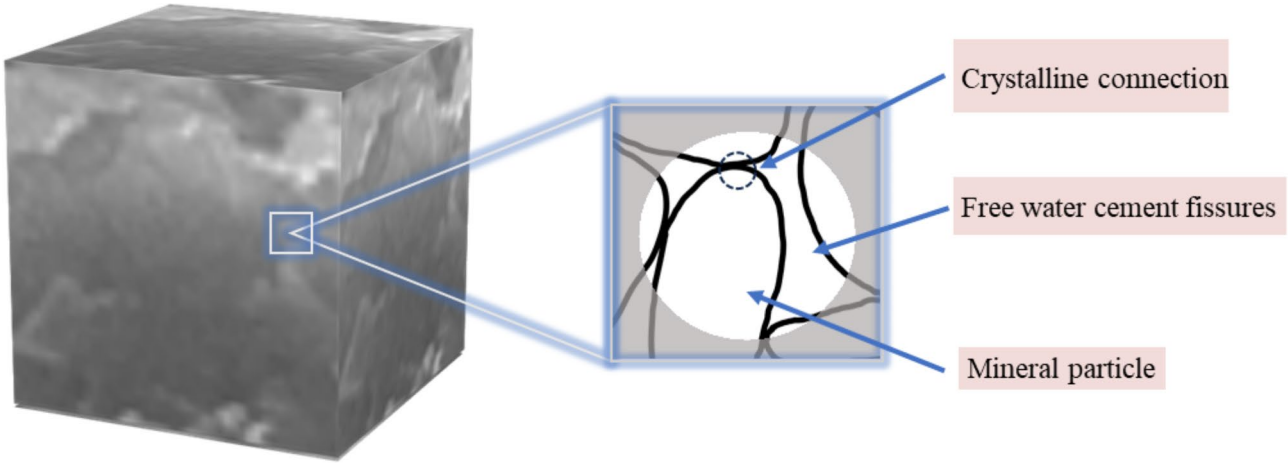

Fig. 16. Schematic diagram of the microstructure of the specimen at 25 °C.

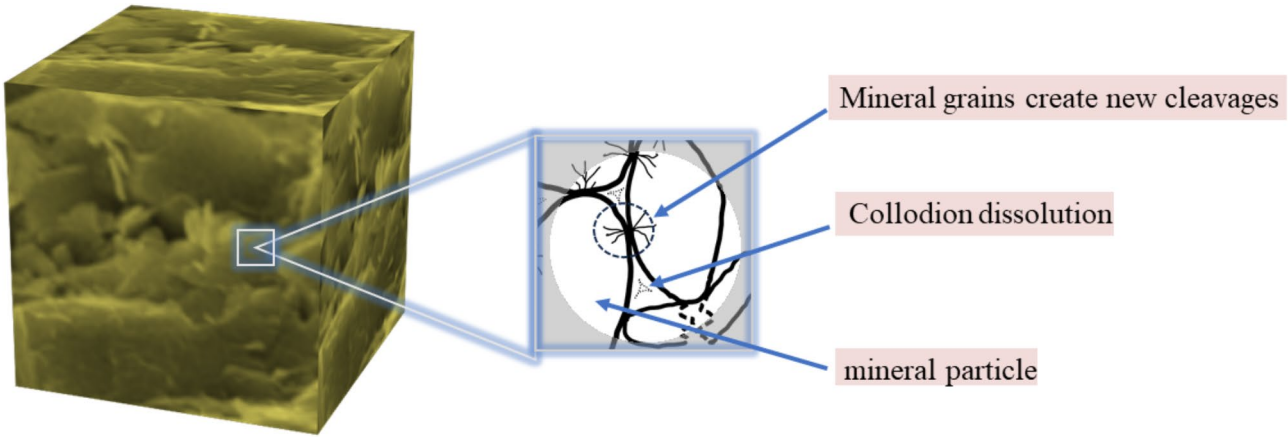

Fig. 17. Schematic diagram of the microstructure of the specimen after high temperature.

sandstone specimen increase and the internal volume increases, resulting in changes in the microstructure and macroscopic physical and mechanical properties of the rock.

Rock is composed of a variety of mineral particles and aggregates. The mechanical properties of rocks are inevitably affected by the group of rock minerals, structure, this is due to the rocks in the temperature under the influence of its internal structure changes, this change has physical changes, such as melting, mineral phase transition, mineral fracture, etc.; There are also chemical changes, such as thermal decomposition of minerals and other reactions. Thus, the red sandstone will generate stress concentration between the mineral particles, the internal mineral structure changes, the extension of the cracks. Because the internal cracks of red sandstone always develop along the tip of the pores, through the internal pores and eventually form large cracks.

Combining the SEM results of related scholars on the evolution of cracks in red sandstone after high-temperature action and the XRD test of red sandstone after high temperature conducted in this paper, it is found that, as shown in Figs. 16 and 17, the internal mineral particles of the heated and cooled rock cooled and shrunk, and the cracks connected and expanded, and the cracks became bigger after cooling and shrinking, and the minerals and cementation materials were thermally decomposed or dissolved. The crack contraction phenomenon occurs at 500~600℃, where thermal stress plays a major role in this temperature range, and thermal reactions appear. When the temperature rises from 500 to 1000 °C, the escape of structural water will change the lattice structure, which in turn produces intergranular cracks. Different minerals are subjected to uneven thermal expansion by temperature, and fissure expansion and penetration occur around the mineral crystals, and the damage gradually increases.

The XRD test pointed out that the diffraction peaks of zeolite, plagioclase and montmorillonite gradually disappeared at this stage, and the different coefficients of thermal expansion of various minerals further aggravated the microscopic damage of the red sandstone. Meanwhile, the change of diffraction information caused by the phase transformation of quartz at this temperature also promoted the rapid development of cracks. In addition, with the increase of temperature, the thermal stress is also gradually enhanced, and the above-combined effects lead to the rapid development, growth, and penetration of cracks and pores in the

red sandstone at this temperature interval, especially at 800~ 1000 ℃, the cracks expand particularly rapidly, resulting in a significant reduction in the macroscopic compressive strength of the red sandstone at this stage.

Theoretical model

To be able to construct theoretical models capable of describing quantitative relationships between temperature, mineral composition changes and mechanical properties, it is assumed that (1) all minerals are subjected to the same strain. (2) The individual mineral properties E_i and σ_{fi} are usually regarded as constants. (3) The overall properties are linear combinations of the properties of the components. The Voigt model is introduced.

Modulus of elasticity at different temperatures:

$$E_0 = \sum_i V_i E_i \tag{12}$$

Where E_0 is the overall modulus of elasticity; E_i is the modulus of elasticity of component i ; and V_i is the volume fraction of component i, which is the mass percentage according to the XRD test results. The volume fraction V_i can be calculated from the mass and mineral density:

$$V_i = \frac{\frac{w_i}{\rho_i}}{\sum_j \frac{w_j}{\rho_j}} \tag{13}$$

Where: w_i he mass percentage of mineral i (obtained by quantitative XRD analysis); ρ_i the density of mineral i ;

The Voigt model is commonly used to estimate the undamaged properties of a material, i.e. assuming that the material is free of cracks or other defects. is a theoretical value in an ideal state. The Voigt model can be modified for high temperature environments:

$$E_0 = \sum_i V_i(T) E_i \tag{14}$$

Where, $E_i(T)$: ideally, should vary with temperature, but in practice is often simplified to take the room temperature value. $V_i(T)$: dynamic volume fraction. In red sandstone, the minerals that play a major strength role are quartz and feldspar. The decomposition or phase transformation of the two minerals at high temperatures is expressed by the weight function transformation fraction $f_i(T)$ ($0 \le f_i \le 1$), which is defined as follows according to the XRD data:

$$f_{quartz}(T) = \begin{cases} 0, \ T < 573^\circ C \\ 1, \ T \geqslant 573^\circ C \end{cases} \tag{15}$$

$$f_{feldspar}(T) = \begin{cases} 0, & T < 500^\circ C \\ \frac{T-500}{500}, & 500^\circ C \leqslant T < 1000^\circ C \\ 1, & T \geqslant 1000^\circ C \end{cases} \tag{16}$$

Volume fraction of mineral i as a function of temperature

$$V_i(T) = V_{i0}\left[1 - f_i(T)\right] + V_{i,new} f_i(T) \tag{17}$$

V_{i0}: volume fraction of mineral i in the initial state.

$V_{i,\,new}$: volume fraction of the new phase, indicating the volume fraction of mineral i completely transformed into the new phase.

This is further combined with the damage variable $D(T)$ (reflecting the cumulative effect of microcracks and porosity, $0 \le D \le 1$).

Assumptions (1) Mechanical properties (σ and E) vary with temperature and damage. (2) Temperature change is a quasi-static process, and dynamic effects are ignored. Then, according to the damage mechanics, the modulus of elasticity after damage by high temperature action:

$$E(T) = E_0(T)(1 - D(T)) \tag{18}$$

$$D(T) = 1 - \frac{E(T)}{E_0(T)} \tag{19}$$

$$D(T) = D_{crack}(T) + D_{min}(T) \tag{20}$$

Where, $D(T)$: includes thermal crack damage and mineral transformation damage. Thermal crack damage $D_{crack}(T)$ is caused by thermal expansion mismatch. Mineral transformation damage $D_{min}(T)$ is caused by mineral decomposition or phase transformation. If $D > 1$, take $D = 1$.

Cracks expand rapidly from 800 °C to 1000 °C, and coupled with the crack expansion rate, the damage increases nonlinearly:

$$D_{crack}(T) = k_1(\frac{T-20}{780})^n \tag{21}$$

D_{crack} : Crack rate at different temperatures T, derived from acoustic emission, DIC or high-speed camera.

k_1: scale factor, a combination of inherent material properties and experimental conditions;

n: the degree of nonlinearity of crack extension velocity with temperature. k_1, *n* were fitted by experimental data in the interval from 800 °C to 1000 °C.

780 °C is the critical point where the internal structure of red sandstone changes from "microdamage accumulation" to "rapid crack expansion".

Mineral transformation leads to damage increment:

$$\Delta D_i = k_{2i} f_i(T) \tag{22}$$

$$D_{min}(T) = \sum_i k_{2i} f_i(T) = D(T) - D_{crack}(T) \tag{23}$$

k_{2i}: damage contribution factor for mineral i. The damage variable at temperature T can be obtained according to the formula.

Therefore, the damage variable at temperature T can be obtained according to the above equation:

$$D(T) = k_1\left(\frac{T-20}{780}\right)^n + k_{2i} f_i(T) \tag{24}$$

Cumulative damage variables at temperature *T*:

$$D(T) = \int_{20}^{T} k_1\left(\frac{T-20}{780}\right)^n + k_{2i} f_i(T) dT \tag{25}$$

Peak Stress:

$$\sigma_{f0} = \sum_i V_i \sigma_{fi} \tag{26}$$

Where σ_{f0} is the overall strength and σ_{fi} is the stress per unit volume of component i.

The Voigt model can be modified for high temperature environments:

$$\sigma_{f0} = \sum_i V_i(T) \sigma_{fi} \tag{27}$$

Where $\sigma_{fi}(T)$: ideally, it should vary with temperature, but in practice it is often simplified to take the room temperature value.

The free expansion strain for thermal crack damage is:

$$\varepsilon_{\mathrm{th}} = \alpha \boldsymbol{\Delta} T \tag{28}$$

$$\Delta T = T - T_0 (T_0 = 20^{\circ} C) \tag{29}$$

The coefficient of thermal expansion, α, is a characteristic parameter of a material's length or volume expansion in response to a change in temperature, and each mineral attempts to expand at different rates when the temperature rises. Mineral particles are constrained from expanding freely by cements or other particles restraining each other. This constraint results in an expansion mismatch that translates into internal stresses.

Hence, thermal stresses:

$$\sigma_{fi} = E_i \alpha_i \Delta T \tag{30}$$

E: local modulus of elasticity;

α: coefficient of thermal expansion

$$\sigma_{f0}(T) = \sum_i V_i(T) \cdot E_i \cdot \alpha_i \cdot \Delta T \tag{31}$$

According to damage mechanics:

Peak Stress and Modulus of Elasticity

$$\sigma_f(T) = \sum_i [V_{i0}(1 - f_i(T)) + V_{i,new} f_i(T)] E_i \alpha_i \Delta T \left[1 - k_1 \left(\frac{T - 20}{780}\right)^n + k_{2i} f_i(T)\right] \tag{32}$$

$$E(T) = E_0(T) \left[1 - k_1 \left(\frac{T - 20}{780}\right)^n + k_{2i} f_i(T)\right] \tag{33}$$

The model systematically reveals the micro-mechanism of the degradation of mechanical properties of red sandstone under high temperature and connects temperature, mineral change and mechanical properties through quantitative relationships, providing a theoretical basis for the study of rock behavior under high-temperature environments.

Conclusion

(1) As the red sandstone has physical changes in the influence of temperature, such as mineral fracture, etc., there will be a concentration of stress between the mineral particles, and the internal cracks will develop along the pore tips to form larger cracks. At the same time, because of the different coefficients of thermal expansion of different minerals, the thermal stress is different, accelerating the formation and expansion of micro-cracks; There are also chemical changes, such as the thermal decomposition reaction of minerals. After high temperature, the apparent color of the red sandstone sample changes from gray-white to white-red, brown-red and bright red. The quartz is stable, and the diffraction intensity of quartz crystals in the high-temperature sample increases with the increase of temperature up to 600 ℃, and the diffraction intensity of quartz crystals in the sample decreases after the high temperature of 600 ℃. The detrital minerals, such as quartz, usually have high hardness. Clay minerals such as montmorillonite, on the other hand, have significant swelling properties. Therefore, the ratio of detrital minerals to clay minerals is also an important factor affecting the mechanical properties and damage mode of red sandstone.

(2) With the increase of temperature, the peak strength and modulus of elasticity under static and dynamic loading decreased significantly and basically showed a linear relationship, compared with the static stress-strain curve, the dynamic stress-strain curve did not have an obvious compaction phase, and the average peak strength decrease under static loading amounted to 35.6%, and the decrease in elastic modulus amounted to 71.1%. Under dynamic loading, the average peak strength decreased by 47%, and the elastic modulus decreased by 53%; the mass loss rate, volume expansion rate and longitudinal wave velocity decay rate under static and dynamic loading showed positive correlation with temperature, and it can be found that the growth was flat below 600℃, and the internal structure of the red sandstone was damaged to a low degree by high temperature in this temperature range. Meanwhile, all the changes increase above 600℃. At 1000℃, the increase reaches 5.76%, 3.5% and 76.92%, respectively, compared with the room temperature.

(3) Under static loading, rocks have time to adapt to changes in external loads. The red sandstone has a more uniform damage pattern. It exhibits cleavage damage accompanied by brittle fracture. The shear surface is conical and shows longitudinal cracks parallel to the loading direction, along with a large amount of pulverized material with obvious friction marks. The higher the temperature, the more serious the damage of the specimen. Among them, 500 ~ 600℃ because the synergistic effect of α-quartz phase transition and clay mineral dehydration exacerbated the non-uniform extension of microcracks, and the gap in the degree of destruction was obvious. At 1000℃, the rock is damaged in the state of powder and small fragments accumulation. This leads to the peak strength and modulus of elasticity under static loading will change with the increase of temperature, but it is relatively smooth.

Under dynamic loading, the rock is unable to adapt to the changes in external loads in time, which leads to more drastic damage. The damage pattern is usually characterized by tensile damage, and the damage process is more rapid and unpredictable. The degree of fragmentation shows a tendency of decreasing and then gradually increasing with increasing temperature. At temperatures above 900 °C, a cleavage surface along the axial direction appears, and the damage degree of the specimen begins to intensify, breaking into a large number of fragments around the specimen, and at 1000 °C, the specimen breaks into smaller fragments. However, at 500 and 800 ℃, the specimen rupture broken degree is reduced. Especially at high temperatures, the dynamic loading led to a sharp decrease in the strength and modulus of elasticity of the rock.

(4) By coupling mineral change, thermal stress and damage evolution, this paper constructs a systematic theoretical model to explain the degradation mechanism of mechanical properties of red sandstone under idealized high temperature action, and realizes the quantitative description of temperature, mineral composition and mechanical properties. In the future, the mechanical response differences of red sandstone under dynamic loading conditions can be explored through in-depth study of the decomposition kinetics of different minerals and their specific effects on the microstructure, and numerical simulations can be introduced to improve the model.

(5) The study focused on 500–1000 °C and also combined the effects of static and dynamic loads. Through microscopic analysis, the changes of mineral composition and other changes of red sandstone after high temperature and loading were explored. Combined with the macro-mechanical property tests, the connection between microstructure and macro-mechanical properties was established, and a systematic theoretical model was constructed, but the research samples could not fully represent all types of red sandstone, so the results have some limitations. In addition, there are differences between laboratory conditions and real engineering environments, and the dynamic loads in real engineering are often more complex and variable, and the results of the study need to be further verified and adjusted when applied to real engineering.

Data availability

Data supporting the results of the study can be accessed upon reasonable request from the corresponding author.

Received: 31 October 2024; Accepted: 11 March 2025
Published online: 04 April 2025

References

1. Meng, Q. et al. Analysis of triaxial compression deformation and strength characteristics of limestone after high temperature. *Arab. J. Geosci.* **13**, (2020).
2. Shi, X. et al. Investigation on physical and mechanical properties of bedded sandstone after high-temperature exposure. *B Eng. Geol. Environ.* **79**, 2591–2606 (2020).
3. Li, Y., Zhai, Y., Wang, C., Meng, F. & Lu, M. Mechanical properties of Beishan granite under complex dynamic loads after thermal treatment. *Eng. Geol.* **267**, (2020).
4. Wang, Z. L., Shi, H. & Wang, J. G. Mechanical behavior and damage constitutive model of granite under coupling of temperature and dynamic loading. *Rock. Mech. Rock. Eng.* **51**, 3045–3059 (2018).
5. Wong, L. N. Y., Li, Z., Kang, H. M. & Teh, C. I. Dynamic loading of carrara marble in a heated state. *Rock. Mech. Rock. Eng.* **50**, 1487–1505 (2017).
6. Shu, R., Yin, T., Li, X., Yin, Z. & Tang, L. Effect of thermal treatment on energy dissipation of granite under cyclic impact loading. *T. Nonferr. Metal Soc.* **29**, 385–396 (2019).
7. Mao, R., Mao, X., Zhang, L. & Liu, R. Effect of loading rates on the characteristics of thermal damage for mudstone under different temperatures. *Int. J. Min. Sci. Techno.* **25**, 797–801 (2015).
8. Ping, Q., Zhang, C., Su, H. & Zhang, H. Experimental study on dynamic mechanical properties and energy evolution characteristics of limestone specimens subjected to high temperature. *Adv. Civ. Eng.* **2020**, (2020).
9. Ping, Q., Wu, M., Yuan, P., Su, H. & Zhang, H. Dynamic splitting experimental study on sandstone at actual high temperatures under different loading rates. *Shock Vib.* **2020**, (2020).
10. Ping, Q., Fang, Z., Ma, D. & Zhang, H. Coupled static-dynamic tensile mechanical properties and energy dissipation characteristic of limestone specimen in Shpb tests. *Adv. Civ. Eng.* **2020**, (2020).
11. Ping, Q., Zhang, C., Sun, H. & Han, X. Dynamic mechanical properties and energy dissipation analysis of sandstone after high temperature cycling. *Shock Vib.* **2020**, (2020).
12. Zhang, R., Ma, D., Su, Q. & Huang, K. Effects of temperature and water on mechanical properties , energy dissipation , and microstructure of argillaceous sandstone under static and dynamic loads. *Shock Vib.* **2020**, (2020).
13. Aibing, J., Shuliang, W. A. N. G. & Yudong, W. E. I. Effect of different cooling conditions on physical and mechanical. *Rock. Soil. Mech.* **41**, 353–3539 (2020).
14. Li, M. & Liu, X. Effect of thermal treatment on the physical and mechanical properties of sandstone: insights from experiments and simulations. *Rock. Mech. Rock. Eng.* **55**, 3171–3194 (2022).
15. Miao, S. & Zhou, Y. Temperature dependence of thermal diffusivity and conductivity for sandstone and carbonate rocks. *J. Therm. Anal. Calorim.* **131**, 1647–1652 (2018).
16. Geng, J. et al. Temperature dependence of the thermal diffusivity of sandstone. *J. Petrol. Sci. Eng.* **164**.
17. Yin, T., Li, Q. & Li, X. Experimental investigation on mode I fracture characteristics of granite after cyclic heating and cooling treatments. *Eng. Fract. Mech.* **222**, 106740 (2019).
18. ULUSAY R. *The ISRM Suggested Methods for Rock Characterization, Testing and Monitoring: 2007–2014* (ed. ULUSAY R.) 51–68 (Springer International Publishing, 2015).
19. China Electricity Council. *GB/T50266-2013 Standard for Test Methods of Engineering Rock Mass* (China Planning Publishing House, 2013).
20. Lili, W. A. N. G. National Defense Industry Press,. Foundation of stress waves. 2nd ed. (ed. Lili, Wang.) 39–64. (2010).
21. Xibing, L. I. & Desheng, G. U. Rock impact dynamics. (ed.Xibing, L.) 12 (Central South University of Technology Press, 1994).
22. Rongrong, Z. & Laiwang, J. Analysis on the fragment and energy dissipation of deep sandstone after high/low temperature treatment in SHPB tests. *J. China Coal Soc.* **43**, 1884–1892 (2018).

Author contributions

H.L. Experimentation, result detection, and writing-original draft preparation; W.L. Experimentation, result detection, data curation; D.Z. Experimentation, writing-original draft preparation.B.C. Literature review, data collation.X.Z. Data collation.

Declarations

Competing interests

The authors declare no competing interests.

Additional information

Correspondence and requests for materials should be addressed to W.L. or X.Z.

Reprints and permissions information is available at www.nature.com/reprints.

Publisher's note Springer Nature remains neutral with regard to jurisdictional claims in published maps and institutional affiliations.